25th ABCM International Congress of Mechanical Engineering
October 20-25, 2019, Uberlândia, MG, Brazil

COB-2019-0872
TOPOLOGICAL DERIVATIVE APPLIED TO THE EIGENVALUE PROBLEM IN A MEMBRANE STRUCTURE

Dirlei Ruscheinsky
Fernando Soares de Carvalho
Carla Tatiana Mota Anflor
Group of Experimental and Computational Mechanics, UnB
dirlei@uft.edu.br; fscarvalho@uft.edu.br; anflor@unb.br

Antônio André Novotny
Laboratório Nacional de Computação Científica, LNCC/MCTI
novotny@lncc.br

Abstract. *During the last years the topological derivative has been developed for a wide range of physical phenomenon modeled by partial differential equations. In this work the topological derivative for the eigenvalue function is derived through the modified Helmholtz equation. The obtained closed form for the topological derivative allows optimizing the membrane structures. In this methodology the first eigenvalue is maximized by using the linear penalty method for volume control. Finally, three example applications are given to substantiate the feasibility of the approaches presented in this paper.*

Keywords: *Topological Derivative, Topological Optimization, Eigenvalue, Membrane.*

1. INTRODUCTION

The control of natural vibration plays an important role in many engineering structures, such as, airplanes, satellites, ships, viaducts, buildings among others. The natural vibration is modeled by solving the eigenvalue and eigenvector of a dynamic problem, where the eigenvalue represents the frequency of the vibration and the eigenvector the modal shape. One of the main goals in a structural dynamic topology optimization is to find a final shape of a structure with the first eigenvalue as higher as possible, resulting in a rigid structure that is able to avoid the resonance when excited in low frequencies. In this sense, the eigenvalues and eigenvectors must be calculated as the topological iterative process evolves during the optimization procedure once the geometry changes in shape and topology. The vibration of a membrane is modeled by the Laplace equation, and in the topological optimization field has been previously studied by Antunes and Freitas (2012, 2016) and Oudet (2004) using techniques such as gradient method and level set, respectively. The topological derivative is classically defined as the first term of the asymptotic expansion of a given shape functional with respect to the parameter associated with the size of an infinitesimal singular perturbation, such as holes, inclusions, source-terms and even cracks introduced at an arbitrary point in a given geometric domain Novotny and Sokolowski (2013). In this work the topological derivative concept will be applied to achieve the best material distribution by maximizing the first eigenvalue. The membrane optimization problem will be solved taking into account the modified Helmholtz equation by calculating the topological derivative for the eigenvalue function, given by,

$$\psi(\chi) := \mathcal{F}_\chi(u) = \frac{\int_\Omega \alpha \|\nabla u\|^2}{\int_\Omega \rho u^2}. \tag{1}$$

2. THE TOPOLOGICAL DERIVATE CONCEPT

For instance, considers an open and bounded domain $\Omega \subset \mathbb{R}^d$, with $d \geq 2$ which is subject to a nonsmooth perturbation confined in a small region $\omega_\varepsilon(\widehat{x})$ of size ε with $\overline{\omega_\varepsilon} \subset \Omega$, as shown in fig. 1. Here, $\widehat{x}$ is an arbitrary point of Ω and ω is a fixed domain of $\mathbb{R}^d$. We introduce a *characteristic function* $x \mapsto \chi(x)$, $x \in \mathbb{R}^d$, associated to the unperturbed domain, namely $\chi = \mathbb{1}_\Omega$, such that

$$|\Omega| = \int_\Omega \chi, \tag{2}$$

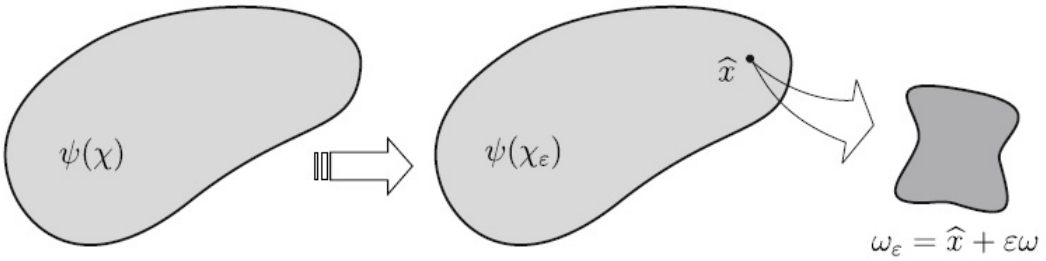

Figure 1: The topological derivative concept

where $|\Omega|$ is the *Lebesgue measure* of Ω.

We define a characteristic function associated to the topologically perturbed domain of the form $x \mapsto \chi_\varepsilon(\widehat{x}, x)$, $x \in \mathbb{R}^d$. The perturbed domain is obtained when a circle-shaped hole $\omega_\varepsilon(\widehat{x})$ (center $\widehat{x}$ and radius ε)) is introduced into the domain Ω. Then this region is populated by an inclusion with different material property from the medium. In particular, a constant function is introduced in parts γ_ε of the form,

$$\gamma_\varepsilon(x) = \begin{cases} 1 & se \quad x \in \Omega \setminus \omega_\varepsilon \\ \gamma & se \quad x \in \omega_\varepsilon \end{cases} , \tag{3}$$

where $\gamma \in \mathbb{R}^+$ is the contrast in the property of the material. In this way, the characteristic function can be represented by $\chi(\widehat{x}) = \mathbf{1}_\Omega - (1-\gamma)\mathbf{1}_{\omega_\varepsilon(\widehat{x})}$. A singular perturbation will be introduced in the differential operator coefficients by contrast γ_ε through the change of material property in the region $w_\varepsilon(\widehat{x}) \subset \Omega$.Therefore, the sensitivity of a shape functional, with respect to the nucleation of a small inclusion can be studied from the concept of topological sensitivity analysis. Then, we assume that a given shape functional, $\psi(\chi_\varepsilon(\widehat{x}))$, associated to the topologically perturbed domain, admits the following topological asymptotic expansion

$$\psi(\chi_\varepsilon(\widehat{x})) = \psi(\chi) + f(\varepsilon)D_T(\widehat{x}) + o(f(\varepsilon)), \tag{4}$$

where $\psi(\chi)$ is the shape functional associated to the reference (unperturbed) domain, $f(\varepsilon)$ is a positive first order correction function of ψ, and $o(f(\varepsilon))$ is the remainder, namely $o(f(\varepsilon))/f(\varepsilon) \to 0$ with $\varepsilon \to 0$. The function, $\widehat{x} \mapsto D_T(\widehat{x})$ is called the topological derivative of ψ at $\widehat{x}$. Essa derivada, pode ser entendida como uma correção de primeira ordem de $\psi(\chi)$ para aproximar $\psi(\chi_\varepsilon(\widehat{x}))$. In fact, after rearranging (4), we have

$$\frac{\psi(\chi_\varepsilon(\widehat{x})) - \psi(\chi)}{f(\varepsilon)} = D_T(\widehat{x}) + \frac{o(f(\varepsilon))}{f(\varepsilon)}. \tag{5}$$

The limit passage $\varepsilon \to 0$ in the above expression leads to the general definition for the *topological derivative*

$$D_T(\widehat{x}) = \lim_{\varepsilon \to 0} \frac{\psi(\chi_\varepsilon(\widehat{x})) - \psi(\chi)}{f(\varepsilon)}. \tag{6}$$

3. THE MODIFIED HELMOLTZ EQUATION

Let us consider a problem of eigenvalue and eigenvector from the modified Helmholtz equation. The mathematical model is given by:

$$\left\{ \begin{array}{l} \text{Find } u, \text{ such that} \\ \quad -\mathrm{div}(\alpha\nabla u) + \rho k u = f \quad \text{in} \quad \Omega\,, \\ \quad\quad\quad\quad\quad\quad u = 0 \quad \text{on} \quad \partial\Omega. \end{array} \right. \tag{7}$$

Considering the perturbation presented in Tables 1 to 3 and Figure 2, one can define the perturbed problem.

$$\left\{ \begin{array}{l} \text{Find } u_\varepsilon, \text{ such what} \\ \quad -\mathrm{div}(\alpha_\varepsilon\nabla u_\varepsilon) - \rho_\varepsilon k u_\varepsilon = f_\varepsilon \quad \text{in} \quad \Omega\,, \\ \quad\quad\quad\quad\quad\quad u_\varepsilon = 0 \quad \text{on} \quad \partial\Omega \\ \quad\quad\quad\quad\quad\quad [\![u_\varepsilon]\!] = 0 \\ \quad\quad\quad\quad [\![\rho_\varepsilon\nabla u_\varepsilon]\!]\cdot n = 0 \end{array} \right\} \text{on} \quad \partial B_\varepsilon\,. \tag{8}$$

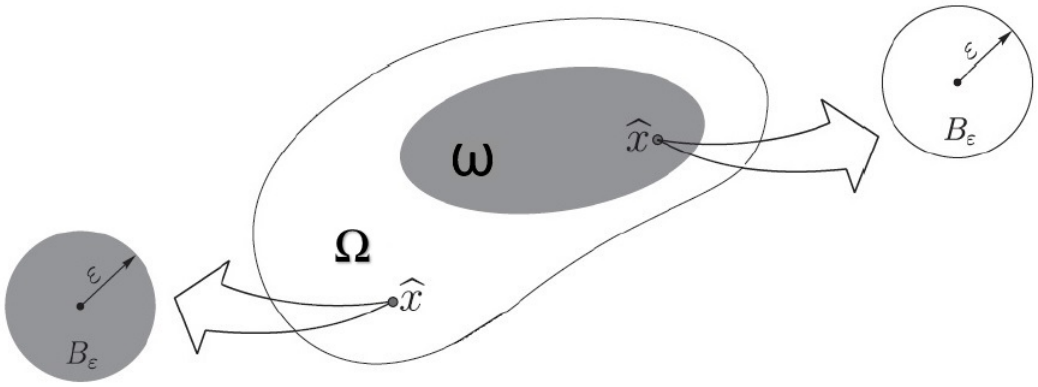

Figure 2: Perturbed domain.

Table 1: Values of α, ρ and f in Ω

	$\alpha(x)$	$\rho(x)$	$f(x)$
$\Omega \setminus \omega$	α_0	ρ_0	f_0
ω	α_1	ρ_1	f_1

Table 2: Values of α_ε, ρ_ε and f_ε in Ω

	α_ε	ρ_ε	f_ε
$\Omega \setminus B_\varepsilon$	α	ρ	f
B_ε	$\gamma_\alpha \alpha$	$\gamma_\rho \rho$	$\gamma_f f$

Table 3: Values of γ_α, γ_ρ and γ_f in Ω

	γ_α	γ_ρ	γ_f
$\Omega \setminus \omega$	$\alpha_1 \alpha_0^{-1}$	$\rho_1 \rho_0^{-1}$	$f_1 f_0^{-1}$
ω	$\alpha_0 \alpha_1^{-1}$	$\rho_0 \rho_1^{-1}$	$f_0 f_1^{-1}$

According to Evans (1998) the smallest eigenvalue associated with the problem (7) is given by Rayleig's formula

$$\lambda = \inf_{u \in H_0^1(\Omega)} \frac{\int_\Omega \alpha \|\nabla u\|^2}{\int_\Omega \rho k(u)^2} = \frac{\mathcal{J}(u)}{\mathcal{G}(u)}. \tag{9}$$

Thus, considering the auxiliary shape functional defined by,

$$\mathcal{G}(u) = \int_\Omega \rho k(u)^2 \qquad \text{and} \qquad \mathcal{J}(u) = \int_\Omega \alpha \|\nabla u\|^2, \tag{10}$$

we can calculate the derived topology to shape functional eigenvalue associated with the unperturbed domain, given by

$$\psi(\chi) := \mathcal{F}_\chi(u) = \frac{\int_\Omega \alpha \|\nabla u\|^2}{\int_\Omega \rho k(u)^2} = \frac{\mathcal{J}(u)}{\mathcal{G}(u)}. \tag{11}$$

4. TOPOLOGICAL DERIVATIVE

The topological derivative of the shape functional presented in (10) is given by,

$$D_T(\mathcal{G}) = -2\alpha \mathbf{P}_\alpha \nabla u \cdot \nabla p - \gamma_\rho \rho k u (u + p) + \gamma_f f p, \tag{12}$$

$$D_T(\mathcal{J}) = -2\alpha \mathbf{P}_\alpha \nabla u \cdot (\nabla u + \nabla q) - \gamma_\rho \rho k u q + \gamma_f f q. \tag{13}$$

where p e q, are solutions of the adjoint problem

$$p \in \mathcal{U}(\Omega) : \int_\Omega \rho \nabla p \cdot \nabla \eta - \int_\Omega \lambda \rho k p \eta = -2 \int_\Omega \rho \nabla u \cdot \nabla \eta = -2\lambda \int_\Omega \rho k u \eta \quad \forall \eta \in \mathcal{U}(\Omega). \tag{14}$$

$$q \in \mathcal{U}(\Omega) : \int_\Omega \rho \nabla q \cdot \nabla \eta - \int_\Omega \lambda \rho k q \eta = -2 \int_\Omega \rho k u \eta \quad \forall \eta \in \mathcal{U}(\Omega). \tag{15}$$

and the polarizing tensor $\mathbf{P}_\alpha$ is given by the following isotropic tensor, $\mathbf{P}_\alpha = \frac{1-\gamma_\alpha}{1+\gamma_\alpha}\mathbf{I}$, ($\mathbf{I}$ is the second-order identity tensor).

The topological asymptotic expansion (Eq. 4), of the functional presented in (11), is given by

$$\psi(\chi_\varepsilon(\widehat{x})) = \psi(\chi) - \pi \varepsilon^2 \frac{-2\alpha \mathbf{P}_\alpha \nabla u \cdot \nabla u + (1 - \gamma_\rho)\rho \lambda k(u)^2}{\mathcal{G}(u)} + o(\varepsilon^2) \tag{16}$$

Taking $f(\varepsilon) = \pi \varepsilon^2$, the following equation for the topological derivative arises,

$$D_T(\widehat{x}) = -\frac{-2\alpha \mathbf{P}_\alpha \nabla u \cdot \nabla u + (1 - \gamma_\rho)\rho \lambda k(u)^2}{\mathcal{G}(u)}. \tag{17}$$

5. NUMERICAL RESULTS

Using the linear penalty method for volume control, the optimization problem we wish to solve is:

$$\text{Minimize} \quad \mathcal{F}_\Omega := \mathcal{F}_\chi(u) + \xi|\Omega|. \tag{18}$$

In equation (18), $\xi > 0$ is a fixed multiplier that imposes a restriction on the volume of elastic material. Since the problem is linear, the topological derivative of (18) is given by,

$$D_T(\mathcal{F}_\Omega) = D_T(\mathcal{F}_\chi(u)) + \xi. \tag{19}$$

For this problem the topological derivative provides the descent direction of the shape function and, consequently, leads to the solution of the problem.

The topology optimization algorithm based on the topological derivative together with a level-set domain representation method is presented. It has been proposed by (Amstutz and Andrä (2006), Giusti *et al.* (2008), Amstutz (2011), Lopes *et al.* (2015)) and consists basically in looking for a local optimality condition for the optimization problem (18), written in terms of the topological derivative and a level-set function.

Two stopping criteria were considered in the present algorithm: $\theta < 1^\circ$ (angle between the level-set function and an auxiliary function g) and the parameter $\kappa < 10^{-3}$ (plays the role of step size in level-set function and $\kappa \in (0, 1]$). In this paper the first stopping criterion has always been reached.

The hold-all domain is discretized by using linear triangular finite elements resulting in an initial uniform mesh with 490.000 elements and 245.701 nodes. In order to increase the accuracy as well as the topology smoothness three steps of mesh refinement during the iterative process were allowed. After the third refinement the mesh is updated resulting with $31.360.000$ elements and $15.685.601$ nodes. In order to illustrate the mesh initial configuration appearance Figure (3) illustrates a square domain 1x1 discretized by a coarse mesh with 100 elements and 61 nodes.

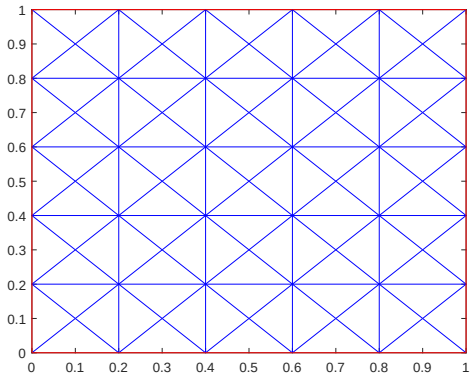

Figure 3: Example: mesh with 100 elements and 61 nodes.

Example 1 *In the initial domain (unit side rectangle), the* $(\partial\Omega)$ *boundaries are set as* $u = 0$*, while the contrast in the property of the material is set as* $\gamma_\alpha = \rho_\alpha = 10^{-3}$*. In order to evaluate the influence of the parameter* ξ *and* k *on the final design a set of three cases whit different values were considered.*

Case 1: In this case we have no concentrated mass source ($k = 0$). In addition, we consider four values for ξ, which are:

Case 1.A: $\xi = 0.1$; **Case 1.B**: $\xi = 0.2$ **Case 1.C**: $\xi = 0.4$ **Case 1.D**: $\xi = 0.8$

The first model of vibration and its respective topological derivative for λ_0 are illustrated according to Figure 4. In addition, the algorithm removes material where the topological derivative assumes the highest values.

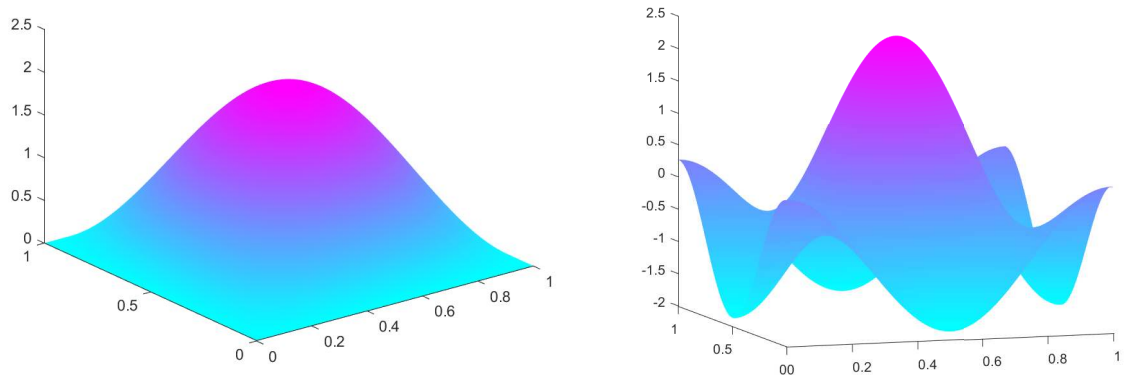

(a) (b)

Figure 4: (a) First mode of vibration; (b) Topological derivative for λ_0.

The eigenvalue and the volume fraction history as the process evolves are shown in Figure 5 for each case under evaluation.

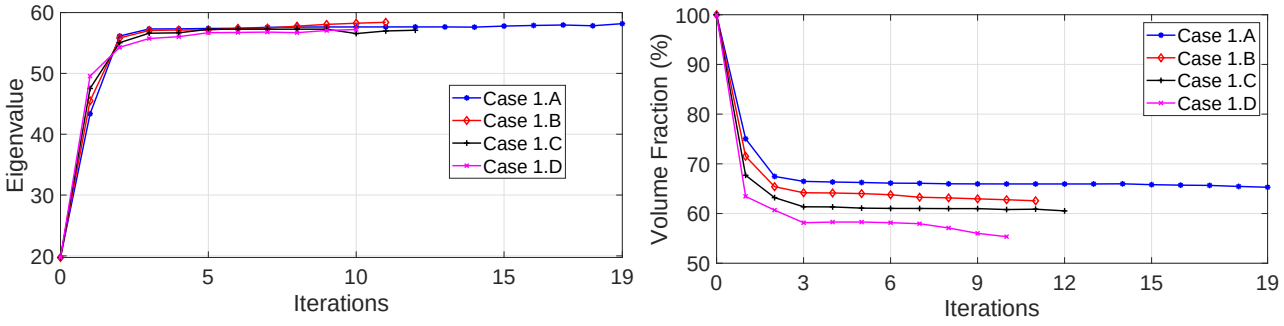

(a) (b)

Figure 5: (a) Eigenvalue; (b) Volume fraction

In spite of the parameter ξ influences on the volume fraction it seems that the eigenvalue converges to the same value for all cases. The percentage differences obtained for all cases are summarized according to Table 4.

Table 4: Eigenvalue, Final volume and Angle θ of the optimized topology

	Case 1.A	Case 1.B	Case 1.C	Case 1.D
Eigenvalue	58.1741	58.3994	57.0929	57.2137
Volume fraction (%)	$65,2888$	$62,5624$	$60,0533$	$55,3394$
Angle θ	$0.6533°$	$0.6011°$	$0.6362°$	$0.4979°$

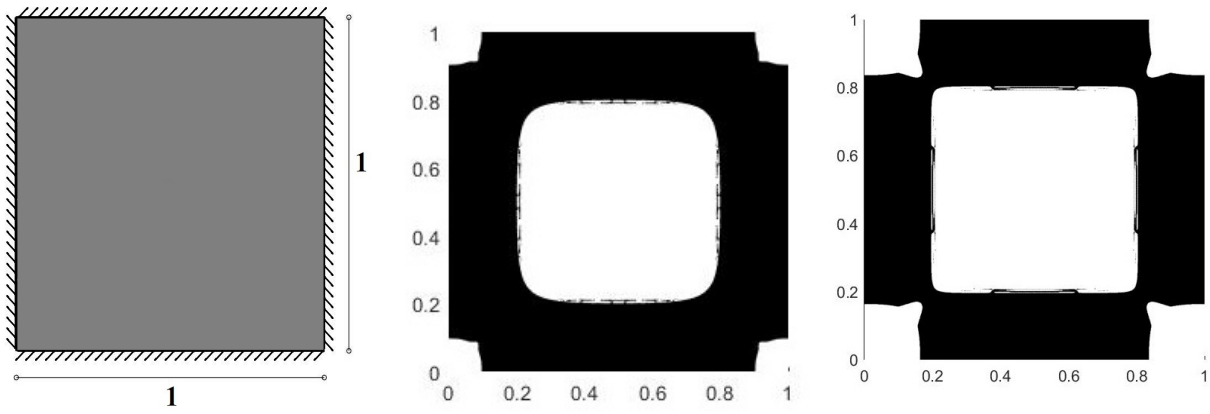

(a) Initial domain (b) Optimized domain for case 1.B, (c) Optimized domain for case 1.D

Figure 6: Initial domain and optimized geometries

Case 2: The mass source is concentrated at point $(0.5, 0.5)$ and $\xi = 0.4$. For this case four values for k were considered,

Case 2.A: $k = 0.02$; **Case 2.B**: $k = 0.1$ **Case 2.C**: $k = 0.15$ **Case 2.D**: $k = 0.2$

Figure 5 depicts the eigenvalue and volume fraction values evolution at each iteration.

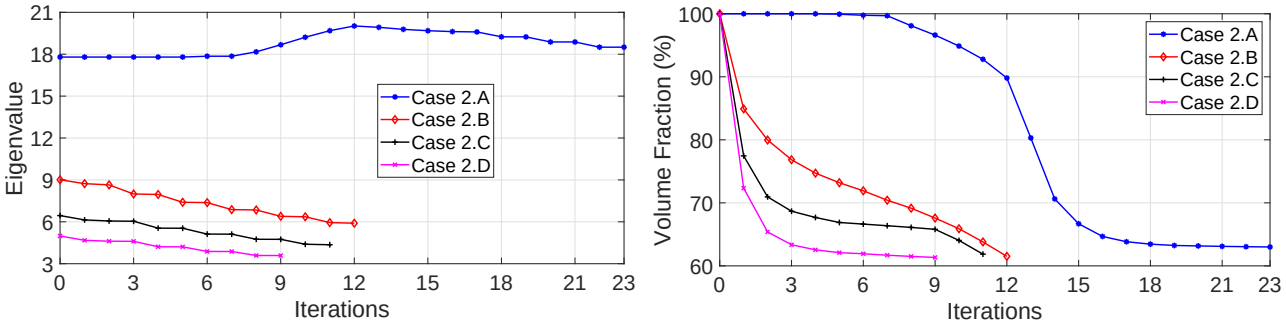

(a) (b)

Figure 7: (a) Eigenvalue; (b) Volume fraction

Table 5 presents the percentage difference obtained for the eigenvalue, volume fraction and angle (θ) for each case. Figure 8 presents the final resulting topologies for the cases 2.A and 2.D. According to Fig. 7 and Fig. 8 it can be seen that the parameter k affects the final shape resulted, in spite of the final volume be the same for both cases.

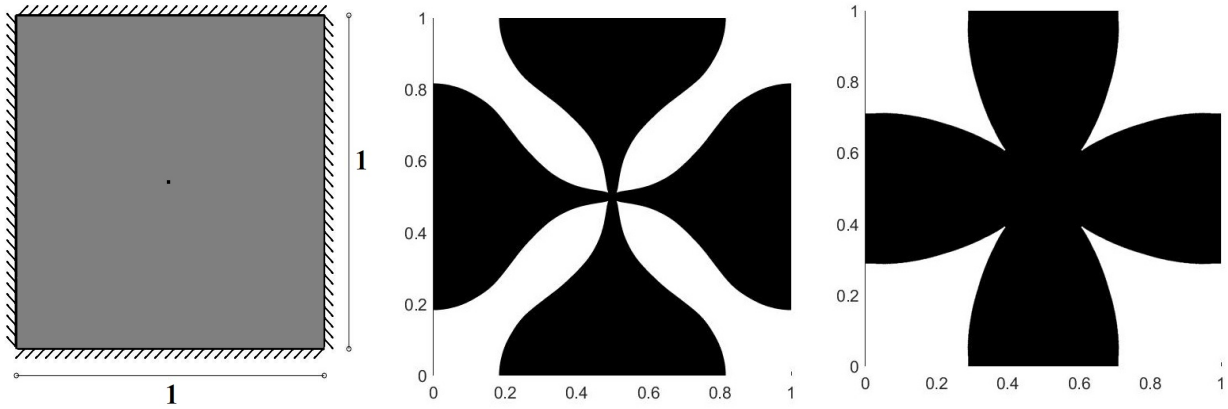

(a) Initial geometry (b) Optimized domain for case 2.A (c) Optimized domain for case 2.D

Figure 8: Initial domain and the optimized domains

Table 5: Eigenvalue, Final volume and Angle θ of the optimized topology

	Case 2.A	Case 2.B	Case 2.C	Case 2.D
Eigenvalue	$18,5033$	$5,8997$	$4,3578$	$3,5882$
Volume fraction $(\%)$	$62,9963$	$61,5128$	$61,8616$	$61,4996$
Angle θ	$0,0310°$	$0,0180°$	$0,0242°$	$0,0082°$

Case 3:For this case a mass source is concentrated at point $(0.5, 0.5)$ and the parameter is set as $k = 0.04$. Five values of parameter ξ were considered,

Case 3.A: $\xi = 0.2$; **Case 3.B**: $\xi = 0.4$ **Case 3.C**: $\xi = 0.6$ **Case 3.D**: $\xi = 0.8$ **Case 3.E**: $\xi = 1.0$

Figure 9 presents the eigenvalue and volume fraction as the iterative process evolves. Table 6 presents the percentage difference for the eigenvalue, volume fraction and θ for all cases. Based on Fig. 9 and Tab. 6 its possible to check the strong influence of the parameter ξ on the eigenvalue results as well as on the volume fraction. Figure 10 depicts the final topology for cases 3.A, 3.C and 3.E, showing the topological difference among them.

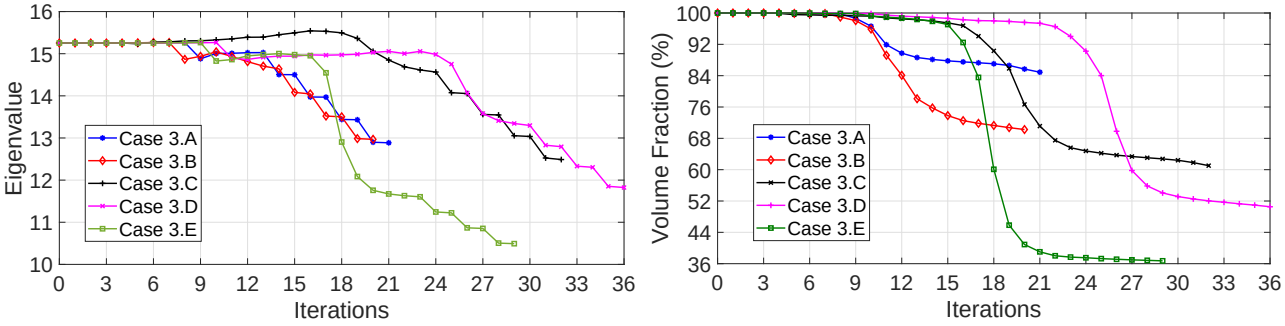

(a) (b)

Figure 9: (a) Eigenvalue; (b) Volume fraction

Table 6: Eigenvalue, Final volume and Angle θ of the optimized topology

	Case 1.A	Case 1.B	Case 1.C	Case 1.D	Case 1.E
Eigenvalue	$13,4332$	$12,9679$	$12,4880$	$11,8240$	10.4918
Volume fraction $(\%)$	$86,6098$	$70,2470$	$60,0533$	$50,5353$	36.7244
Angle θ	$0.0104°$	$0.0224°$	$0.0329°$	$0.0351°$	$0.0354°$

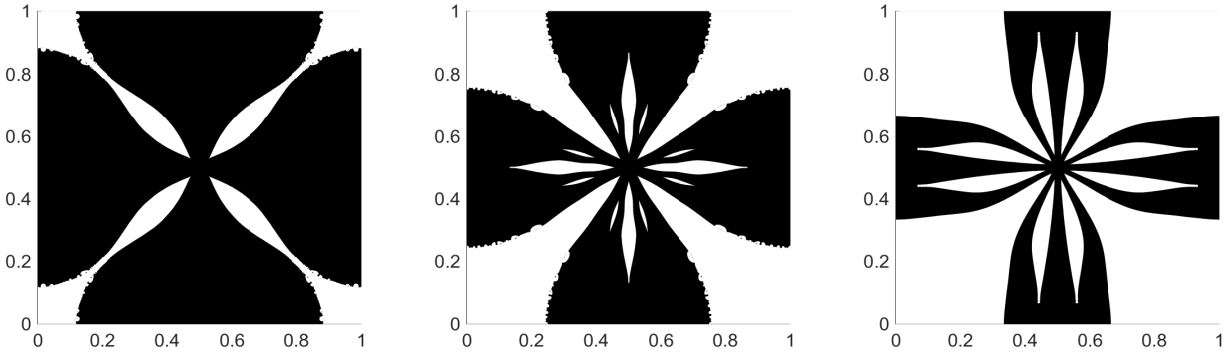

(a) Optimized domain for case 3.A (b) Optimized domain for case 3.C (c) Optimized domain for case 3.E

Figure 10: Optimized domains

6. CONCLUSIONS

The topological derivative for the eigenvalue function was calculated considering the modified Helmholtz equation. The main goal was to maximize the first eigenvalue by removing/adding material. For the optimization procedure a routine was written based on level-set domain representation and a linear penalty method for volume control was used. The influence of the parameters k and xi on the final topology were also investigated. Several examples were presented in order to demonstrate the feasibility in resulting topologies with the first eigenvalue maximized.

7. REFERENCES

Amstutz, S., 2011. "Analysis of a level set method for topology optimization". *Optimization Methods and Software*, Vol. 26, No. 4-5, pp. 555–573.

Amstutz, S. and Andrä, H., 2006. "A new algorithm for topology optimization using a level-set method". *Journal of Computational Physics*, Vol. 216, No. 2, pp. 573–588.

Antunes, P. and Freitas, P., 2012. "Numerical optimization of low eigenvalues of the dirichlet and neumann laplacians". *Journal of Optimization Theory and Applications*, Vol. 154 (1), pp. 235–257.

Antunes, P. and Freitas, P., 2016. "Optimisation of eigenvalues of the dirichlet laplacian with a surface area restriction". *Applied Mathematics & Optimization*, Vol. 73 (2), pp. 313 – 328.

Evans, L.C., 1998. *Partial Differential Equations*. American Mathematical Society, Providence,.

Giusti, S.M., Novotny, A.A. and C., P., 2008. "Topological sensitivity analysis of inclusion in two-dimensional linear elasticity". *Engineering Analysis with Boundary Elements*, Vol. 32, No. 11, pp. 926 – 935.

Lopes, C.G., Santos, R.B. and Novotny, A.A., 2015. "Topological derivative-based topology optimization of structures subject to multiple load-cases". *Latin American Journal of Solids and Structures*, Vol. 12, No. 5, pp. 834–860.

Novotny, A.A. and Sokolowski, J., 2013. *Topological derivatives in shape optimization. Interaction of Mechanics and Mathematics*. Springer, Berlin.

Oudet, E., 2004. "Numerical minimization of eigenmodes of a membrane with respect to the domain". *ESAIM. Control, Optimisation and Calculus of Variations*, Vol. 10, No. 3, pp. 315–330.